ISME

Free Vibration Analysis of Functionally Graded Rectangular Plates via Differential Quadrature Method

M. Talley *
M.Sc. Student

A. R. Khorshidvand †
Assistant Professor

In this study, free vibration of functionally graded (FG) rectangular plates for various types of boundary conditions has been presented. The properties of the plate are assumed as power-law form along the thickness direction, while poisson's ratio is kept constant. The governing equations of motion are derived based on Mindlin plate theory. The numerical solution, differential quadrature method (DQM) is used to discretized the system of partial differential equations and boundary conditions. The numerical results on natural frequencies of the FG plate for combination of boundary conditions, volume fraction index, radii to thickness, and aspect ratio are presented and with existing results in the literature are compared.

Keywords: Differential quadrature method, Free vibration, Functionally graded, Rectangular plates, Mindlin plate theory

1 Introduction

Functionally graded materials (FGMs) are designed so that material properties vary smoothly and continuously through the thickness from the surface of a ceramic exposed to high temperature to that of a metal on the other surface [1].
Many researches on analysis of free and forced vibration of plate-type structures have been reported. Leissa [2,3] studied on free vibration of rectangular isotropic plates based on the classical Kirchhoff-Love hypothesis. The analysis of plate was considered in combinations of simply supported (S), clamped (C), and free (F) edge conditions. Gorman [4] obtained the exact solutions for the free in-plane vibration of rectangular plates for two distinct types of simply supported boundary conditions. where the boundary condition was two opposite edges simply supported while the other two edges are both clamped or both free. Matsunaga [5] employed power series expansion for displacement components in conjunction with Hamilton's principles to evaluate the natural frequency of uniform thick plates with simply supported edges. Rui Li et al. [6] presented a developed symplectic superposition method for free vibration problems. They obtained a general set of equations for determining the natural frequencies and mode shapes of the plates with any point supports. Fallah et al. [7] studied free vibration of moderately thick rectangular FG plates resting on Winkler model elastic foundation with various combinations of

* M.Sc. Student, Department of Mechanical Engineering, South Tehran Branch, Islamic Azad University, Tehran, Iran, talleymohammad@gmail.com
† Corresponding Author, Assistant Professor, Department of Mechanical Engineering, South Tehran Branch, Islamic Azad University, Tehran, Iran, ar_khorshidvand@azad.ac.ir
Manuscript received April 30, 2018; revised June 29, 2018; accepted July 14, 2018.

boundary conditions. They obtained governing equations of motion based on the Mindlin plate theory and presented a semi-analytical solution using the extended Kantorovich method. Y.F. Xing, T.F. Xu, [8] presented the exact solutions of three configurations (G-G-C-C, SS-G-C-C and C-C-C-G) for the first time by using separation of variables method for free vibrations of orthotropic rectangular thin plates.

The differential quadrature method in compared with the finite element method and finite difference methods, in addition to the its ease of use and implementation, it can generate numerical results with high-order of accuracy by using a considerably smaller number of grid points and therefore requiring relatively little computational effort [9,10].
The differential quadrature method, which was first introduced by Bellman and his associates [11,12],as a discretization technique for solving directly the governing equations is used in engineering and mathematics. It approximates the derivative of a function, with respect to a variable at a given grid point, by a weighed linear summation of the function values at all of the grid points in the domain of that variable. Malekzadeh and Karami [13] used DQM for free vibration analysis of thick plates with variable thickness on two-parameter elastic foundation. Ferreira et al. [14] combined the generalized DQM with the Carrera Unified Formulation to predict the static deformations and the free vibration behavior of thin and thick isotropic as well as cross-ply laminated plates. They showed that proposed methodology to be able to deal not only with fully clamped or completely simply-supported boundary conditions, but also with clamped, supported or free mixed external conditions. Rui Li et al. [15] obtained accurate analytic solutions for free vibration of rectangular thick plates with an edge free. They used for first time an up-to-date rational superposition method in the symplectic space for thick plates free vibration. P. Malekzadeh and S.M. Monajjemzadeh [16] obtained the nonlinear dynamic response of thin FG plates under concentrated moving load using the finite element method. First, they derived the nonlinear equations of motion based on the Classical Plate Theory by utilizing Hamilton's principle and then, employed Newmark's time integration scheme in conjunction with Newton-Raphson method. S.A. Eftekhari, A.A. Jafari [17] presented a mixed Ritz-DQ method to study the free and forced vibration of rectangular plates. They reported numerical results of their studies for various type of boundary conditions and concluded the presented method has more efficiency and accuracy than other numerical methods.

In this paper, the linear vibration equations of functionally graded rectangular plates are derived based on Mindlin plate theory by using Hamilton's principle. The influence of transverse shear and rotary inertia is taken into account. The researcher have applied eighth boundary conditions which are all forms that can be considered deploying simply supported (S), clamped (C), and free (F) on these plates. The effect of volume fraction index n FG materials on natural frequency in combination of different boundary conditions for some aspect ratio is investigated. This appears to be the first thorough study by using DQM and based on Mindlin plate theory that presents effects of boundary conditions, material, and geometrical parameters on natural frequencies of FG rectangular plates.

2 Problem Formulation

Consider an FG rectangular plate of length a, width b, and a uniform thickness h as shown in Fig. (1). The plate is referred to a Cartesian coordinate system (x,y,z) with the co-ordinates x, and y along the in-plane directions and z in thickness direction, positive downward. Here, it is assumed that the material properties (i.e., Young's modulus E and density ρ) of the FG plate vary through the plate's thickness according to power-law function for the volume fraction of the constituents which introduced by Wakashima et al. as follows: [18]

$$P\left(z\right) = P_m + \left(P_c - P_m\right)\left(\frac{z}{h} + \frac{1}{2}\right)^n \tag{1}$$

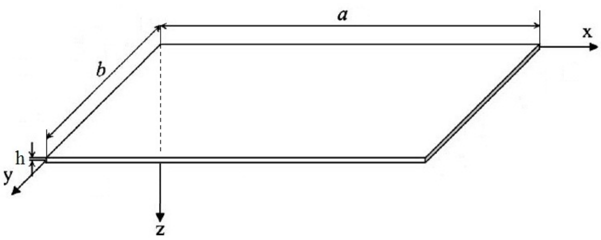

Figure 1 The geometry of FGM plate

In which $P(z)$ denotes a typical material property $(E;\rho)$, P_c and P_m refer to ceramic and metal constituents, respectively, and n which is called volume fraction index and is a parameter describing the material variation profile through the thickness of the FG plate.

Displacement field of rectangular plate in the Cartesian coordinate system according to Mindlin's assumptions may be written as:

$$u_1\left(x,y,z,t\right)=-z\theta_x\left(x,y,t\right) \tag{2}$$

$$u_2\left(x,y,z,t\right)=-z\theta_y\left(x,y,t\right) \tag{3}$$

$$u_3\left(x,y,z,t\right)=w\left(x,y,t\right) \tag{4}$$

where u_1 and u_2 are the in-plane displacements of plate in x-, and y- directions, and u_3 is its lateral deflection. θ_x and θ_y present the transverse normal rotation about the x-, and y- axes.
Using equations (2)–(4), the linear strain components can be written as:

$$\varepsilon_{xx}=\frac{\partial u_1}{\partial x} \tag{5}$$

$$\varepsilon_{yy}=\frac{\partial u_2}{\partial y} \tag{6}$$

$$\gamma_{xy}=\frac{\partial u_1}{\partial y}+\frac{\partial u_2}{\partial x} \tag{7}$$

$$\gamma_{xz}=\frac{\partial u_1}{\partial z}+\frac{\partial u_3}{\partial x} \tag{8}$$

$$\gamma_{yz}=\frac{\partial u_2}{\partial z}+\frac{\partial u_3}{\partial y} \tag{9}$$

Based on Hook's law, for the plane stress case, stress-strain relations are obtained as:

$$\sigma_{xx}=\frac{E(z)}{1-\nu^2}\left(\varepsilon_{xx}+\nu\varepsilon_{yy}\right) \tag{10}$$

$$\sigma_{yy}=\frac{E(z)}{1-\nu^2}\left(\varepsilon_{yy}+\nu\varepsilon_{xx}\right) \tag{11}$$

$$\sigma_{xy}=\frac{E(z)}{2\left(1+\nu\right)}\gamma_{xy} \tag{12}$$

$$\sigma_{xz}=\int\left(\frac{\partial\sigma_{xx}}{\partial x}+\frac{\partial\sigma_{xy}}{\partial y}\right)dz \tag{13}$$

$$\sigma_{yz}=\int\left(\frac{\partial\sigma_{yy}}{\partial y}+\frac{\partial\sigma_{xy}}{\partial x}\right)dz \tag{14}$$

Using Hamilton's principle

$$\int_{t_1}^{t_2}\left(\delta K-\delta U\right)\,dt=0 \tag{15}$$

where δK and δU are the variation of the kinetic energy and potential energy of the FG plate. Potential energy U, the kinetic energy K of the plate are given by:

$$U = \frac{1}{2}\iiint_V \left(\sigma_{xx}\varepsilon_{xx} + \sigma_{yy}\varepsilon_{yy} + \sigma_{xy}\gamma_{xy} + \sigma_{xz}\gamma_{xz} + \sigma_{yz}\gamma_{yz}\right) dV \tag{16}$$

$$K = \frac{1}{2}\iiint_V \rho\, v_0^2\, dV \tag{17}$$

in which v_0 denotes total velocity of each point of plate as:

$$v_0^2 = \sqrt{\dot{w}^2 + \dot{\theta}_x^2 + \dot{\theta}_y^2} \tag{18}$$

By substituting the variation of relations (16) and (17) into equation (15), the governing equations of motion are obtained as:

$$A_{xx}\left[-\kappa\frac{1-\nu}{2}\left(\theta_x + \frac{\partial w}{\partial x}\right)\right] + \tag{19}$$
$$C_{xx}\left[\left(\frac{\partial^2\theta_x}{\partial x^2}\right) + \frac{1-\nu}{2}\left(\frac{\partial^2\theta_x}{\partial y^2}\right) + \frac{1+\nu}{2}\left(\frac{\partial^2\theta_y}{\partial y\partial x}\right)\right] = I_C\frac{\partial^2\theta_x}{\partial t^2}$$

$$A_{xx}\left[-\kappa\frac{1-\nu}{2}\left(\theta_y + \frac{\partial w}{\partial y}\right)\right] + \tag{20}$$
$$C_{xx}\left[\left(\frac{\partial^2\theta_y}{\partial y^2}\right) + \frac{1-\nu}{2}\left(\frac{\partial^2\theta_y}{\partial x^2}\right) + \frac{1+\nu}{2}\left(\frac{\partial^2\theta_x}{\partial x\partial y}\right)\right] = I_C\frac{\partial^2\theta_y}{\partial t^2}$$

$$A_{xx}\left[-\kappa\frac{1-\nu}{2}\left(\frac{\partial^2 w}{\partial x^2} + \frac{\partial^2 w}{\partial y^2} + \frac{\partial\theta_x}{\partial x} + \frac{\partial\theta_y}{\partial y}\right)\right] = I_A\frac{\partial^2 w}{\partial t^2} \tag{21}$$

where

$$A_{xx} = \int \frac{E(z)}{1-\nu^2}\, dz \quad , \quad C_{xx} = \int \frac{E(z)}{1-\nu^2} z^2\, dz$$
$$I_A = \int \rho(z)\, dz \quad , \quad I_C = \int \rho(z) z^2\, dz \tag{22}$$
$$\kappa = \pi^2/12$$

κ is corection factor.

The essential boundary conditions for simply supported, clamped, and free edges of plate are as follows :

Simply supported edge (S)

$$\text{x=0, a} \qquad \theta_y = w = M_x = 0$$
$$\text{y=0, b} \qquad \theta_x = w = M_y = 0 \tag{23}$$

Clamped edge (C)

$$\text{x=0, a} \qquad \theta_x = \theta_y = w = 0$$
$$\text{y=0, b} \qquad \theta_x = \theta_y = w = 0 \tag{24}$$

Free edge (F)

$$\text{x=0, a} \qquad Q_x = M_x = M_{xy} = 0$$
$$\text{y=0, b} \qquad Q_y = M_y = M_{xy} = 0 \tag{25}$$

where M_x, M_y, M_{xy} are moments and Q_x, Q_y are shear force stress resultants respectively.

$$Q_x = \kappa \frac{1-\nu}{2} A_{xx} \left(\frac{\partial w}{\partial x} + \theta_x \right) \tag{26}$$

$$Q_y = \kappa \frac{1-\nu}{2} A_{xx} \left(\frac{\partial w}{\partial y} + \theta_y \right) \tag{27}$$

$$M_x = C_{xx} \left(\frac{\partial \theta_x}{\partial x} + \nu \frac{\partial \theta_y}{\partial y} \right) \tag{28}$$

$$M_y = C_{xx} \left(\frac{\partial \theta_y}{\partial y} + \nu \frac{\partial \theta_x}{\partial x} \right) \tag{29}$$

$$M_{xy} = \frac{1-\nu}{2} C_{xx} \left(\frac{\partial \theta_x}{\partial y} + \frac{\partial \theta_y}{\partial x} \right) \tag{30}$$

3 Differential quadrature method

Let $\psi(x, y)$ be a solution of a differential equation and $0 \leq x_i \leq a$, $0 \leq y_i \leq b$ be a set of sample points in the direction of x-axis and y-axis. According to DQM, the rth-order derivative of the function $\psi(x, y)$ at a point $x = x_i$ along any line $y = y_j$ parallel to the x-axis may be written as [19]

$$\psi^{(r)}|_{x=x_i} = \sum_{k=1}^{N_x} A_{ik}^{(r)} \psi_{kj} \tag{31}$$

and sth-order y-partial derivative at a discrete point $y = y_j$ along any line $x = x_i$ parallel to the y-axis may be written as

$$\psi^{(s)}|_{y=y_j} = \sum_{l=1}^{N_y} B_{jl}^{(s)} \psi_{il} \tag{32}$$

where N_x and N_y are the number of sample points in the direction of x-axis and y-axis, $A_{ik}^{(r)}$ and $B_{jl}^{(s)}$ are the weighting coefficients of the rth-order and sth-order derivative. The weighting coefficients can be determined by the functional approximations in the direction of x and y axis. Using the Lagrange interpolation polynomials as the approximating functions, Quan and Chang obtained the following algebraic formulations to compute the first-order weighting coefficients [20]

$$A_{ik}^{(1)} = \frac{\prod (x_i)}{(x_i - x_k) \prod (x_k)}, \qquad i \neq k, \qquad i, k = 1, 2, \ldots, N_x \tag{33}$$

$$A_{ii}^{(1)} = - \sum_{l=1, l \neq i}^{N_x} A_{il}^{(1)}, \qquad i = k, \qquad i = 1, 2, \ldots, N_x \tag{34}$$

where

$$\prod (x_i) = \prod_{\overline{k}=1, \overline{k} \neq i}^{N_x} \left(x_i - x_{\overline{k}} \right), \qquad \prod (x_k) = \prod_{\overline{k}=1, \overline{k} \neq i}^{N_x} \left(x_k - x_{\overline{k}} \right) \tag{35}$$

The weighting coefficients of the rth-order derivative can be obtained from the following recurrence relationship [19],

$$A_{ik}^{(r)} = r\left[A_{ii}^{(r-1)}A_{ik}^{(r)} - \frac{A_{ik}^{(r-1)}}{x_i - x_k}\right], \qquad i \neq k, \qquad i,k = 1,2,\ldots,N_x \tag{36}$$

$$A_{ii}^{(r)} = -\sum_{l=1,l\neq i}^{N_x} A_{il}^{(r)}, \qquad i = k, \qquad i = 1,2,\ldots,N_x \tag{37}$$

Eqs (33) through (37) are given for the x-partial derivatives; the equations for the y-partial derivatives follow in an identical manner.
One of the key factors in the accuracy and rate of convergence of the DQ solutions is the choice of grid points. It has been suggested that the zeros of some orthogonal polynomials are commonly adopted as non-uniformly spaced grid points can generate more accurate solutions. Bert and Malik firstly introduced grid points for calculation of weighting coefficients as follows [19].

$$x_i = \frac{a}{2}\left[1 - \cos\left(\frac{i-2}{N_x - 1}\pi\right)\right], \qquad y_j = \frac{b}{2}\left[1 - \cos\left(\frac{j-2}{N_y - 1}\pi\right)\right] \tag{38}$$

It was shown that the DQ solutions with this type of sample points produce better accuracy than the commonly used uniform and non-uniform grid points.

4 Dimensionless governing equations

To solve the governing equations (19), (20), and (21), these equations must be obtained in dimensionless form.
To this purpose the following dimensionless parameters can be used as

$$\begin{aligned} &w = W(x,y)e^{i\omega t}, \qquad \theta_x = \Theta_x(x,y)e^{i\omega t}, \qquad \theta_y = \Theta_y(x,y)e^{i\omega t}, \\ &\omega = \Omega\left(C_{xx}/I_A a^4\right)^{1/2}, \qquad t = T(I_A a^4/C_{xx})^{1/2}, \qquad x = Xa, \qquad y = Yb, \\ &\lambda_1 = a/b, \qquad \lambda_2 = a/h \end{aligned} \tag{39}$$

and finally the dimensionless governing equations can be written in the following form

$$\begin{aligned} &\frac{\lambda_2^4 E^*}{\rho^*}\left[-\kappa\frac{1-\nu}{2}\left(\Theta_x + \frac{\partial W}{\partial X}\right)\right] + \\ &\frac{\lambda_2^2}{\rho^*}\left[\left(\frac{\partial^2\Theta_x}{\partial X^2}\right) + \frac{1-\nu}{2}\lambda_1^2\left(\frac{\partial^2\Theta_x}{\partial Y^2}\right) + \frac{1+\nu}{2}\lambda_1\left(\frac{\partial^2\Theta_y}{\partial Y\partial X}\right)\right] = \frac{\partial^2\Theta_x}{\partial T^2} \end{aligned} \tag{40}$$

$$\begin{aligned} &\frac{\lambda_2^4 E^*}{\rho^*}\left[-\kappa\frac{1-\nu}{2}\left(\Theta_y + \lambda_1\frac{\partial W}{\partial Y}\right)\right] + \\ &\frac{\lambda_2^2}{\rho^*}\left[\lambda_1^2\left(\frac{\partial^2\Theta_y}{\partial Y^2}\right) + \frac{1-\nu}{2}\left(\frac{\partial^2\Theta_y}{\partial X^2}\right) + \frac{1+\nu}{2}\lambda_1\left(\frac{\partial^2\Theta_x}{\partial X\partial Y}\right)\right] = \frac{\partial^2\Theta_y}{\partial T^2} \end{aligned} \tag{41}$$

$$K\left(\frac{\partial^2 W}{\partial X^2} + \lambda_1^2\frac{\partial^2 W}{\partial Y^2} + \frac{\partial\Theta_x}{\partial X} + \lambda_1\frac{\partial\Theta_y}{\partial Y}\right) = \frac{\partial^2 W}{\partial T^2} \tag{42}$$

where

$$E^* = \frac{n + \frac{E_c}{E_m}}{(n+1)\left[\frac{1}{12} + \left(\frac{E_c}{E_m} - 1\right)\left(\frac{1}{n+3} - \frac{1}{n+2} + \frac{1}{4(n+1)}\right)\right]}$$

$$\rho^* = \frac{12\left(\frac{\rho_c}{\rho_m} - 1\right)\left(\frac{1}{n+3} - \frac{1}{n+2} + \frac{1}{4(n+1)}\right) + 1}{12\left[1 + \frac{1}{n+1}\left(\frac{\rho_c}{\rho_m} - 1\right)\right]} \tag{43}$$

$$K = -\frac{\kappa\lambda_2^2 E^*(1-\nu)}{2}$$

5 Solving process

Here, the governing equations and boundary conditions are discretized based on differential quadrature technique. To obtain the DQ form of equations, first x and y directions of the plate are discretized to N and M grid points and then governing equations and boundary conditions, via DQ method are discretized as follows:

$$-\frac{\lambda_2^4 E^*}{I_2^*}\left[\kappa\frac{1-\nu}{2}\left(\Theta_{x\,ij} + \sum_{n=1}^{N} c_{in}^{(1)} W_{nj}\right)\right] + \tag{44}$$

$$\frac{\lambda_2^2}{I_2^*}\left[\left(\sum_{n=1}^{N} c_{in}^{(2)}\Theta_{x\,nj}\right) + \lambda_1\frac{1+\nu}{2}\left(\sum_{m=1}^{M}\sum_{n=1}^{N}\bar{c}_{jm}^{(1)}c_{in}^{(1)}\Theta_{y\,mn}\right) + \lambda_1^2\frac{1-\nu}{2}\left(\sum_{m=1}^{M}\bar{c}_{jm}^{(2)}\Theta_{x\,im}\right)\right] = \Omega^2\Theta_{x\,ij}$$

$$\frac{\lambda_2^4 E^*}{I_2^*}\left[\kappa\frac{1-\nu}{2}\left(\Theta_{y\,ij} + \lambda_1\sum_{m=1}^{M}\bar{c}_{jm}^{(1)} W_{im}\right)\right] + \tag{45}$$

$$\frac{\lambda_2^2}{I_2^*}\left[\lambda_1^2\left(\sum_{m=1}^{M}\bar{c}_{jm}^{(2)}\Theta_{y\,im}\right) + \lambda_1\frac{1+\nu}{2}\left(\sum_{n=1}^{N}\sum_{m=1}^{M} c_{in}^{(1)}\bar{c}_{jm}^{(1)}\Theta_{x\,nm}\right) + \frac{1-\nu}{2}\left(\sum_{n=1}^{N} c_{in}^{(2)}\Theta_{y\,nj}\right)\right] = \Omega^2\Theta_{y\,ij}$$

$$K\left[\left(\sum_{n=1}^{N} c_{in}^{(2)} W_{nj}\right) + \lambda_1^2\left(\sum_{m=1}^{M}\bar{c}_{jm}^{(2)} W_{im}\right) + \left(\sum_{n=1}^{N} c_{in}^{(1)}\Theta_{x\,nj}\right) + \lambda_1\left(\sum_{m=1}^{M}\bar{c}_{jm}^{(1)}\Theta_{y\,im}\right)\right] = \Omega^2 W_{ij} \tag{46}$$

and the stress resultunts:

$$Q_{x\,ij} = \kappa\frac{1-\nu}{2}\left(A_{xx}\sum_{n=1}^{N} A_{in}^{(1)} W_{nj} + \Theta_{x\,ij}\right) \tag{47}$$

$$Q_{y\,ij} = \kappa\frac{1-\nu}{2}A_{xx}\left(\lambda_1\sum_{m=1}^{M} B_{jm}^{(1)} W_{in} + \Theta_{y\,ij}\right) \tag{48}$$

$$M_{x\,ij} = C_{xx}\left(\sum_{n=1}^{N} A_{in}^{(1)}\Theta_{x\,nj} + \nu\lambda_1\sum_{m=1}^{M} B_{jm}^{(1)}\Theta_{y\,im}\right) \tag{49}$$

$$M_{x\,ij} = C_{xx}\left(\lambda_1\sum_{m=1}^{M} B_{jm}^{(1)}\Theta_{y\,im} + \nu\sum_{n=1}^{N} A_{in}^{(1)}\Theta_{x\,nj}\right) \tag{50}$$

$$M_{xy\,ij} = \frac{1-\nu}{2}C_{xx}\left(\sum_{n=1}^{N} A_{in}^{(1)}\Theta_{y\,nj} + \lambda_1\sum_{m=1}^{M} B_{jm}^{(1)}\Theta_{x\,im}\right) \tag{51}$$

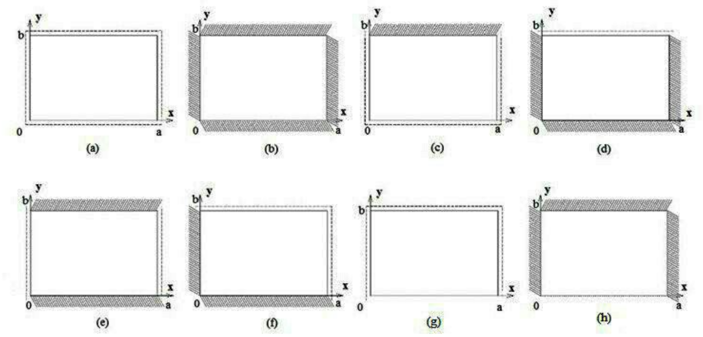

Figure 2 Configurations of combined simply supported ,clamped and free rectangular plates are indicated by (a) SSSS, (b) CCCC, (c) SCSS, (d) CSCC, (e) SCSC, (f) CSSC, (g) SSSF, (h) CCCF. For convenience, S, C and F in a four-letter symbol are denoted as a simply supported, a clamped and free respectively.

According to the governing equations and boundary conditions and by using DQ method, the natural frequencies can be obtained. After a long reformulation, the governing equations and boundary conditions can be converted to the following matrix form [9].

$$\begin{bmatrix} \mathrm{BB} & \mathrm{BD} \\ \mathrm{DB} & \mathrm{DD} \end{bmatrix} \begin{Bmatrix} d_B \\ \Theta_{x\,ij} \\ \Theta_{y\,ij} \\ W_{ij} \end{Bmatrix} = \Omega^2 \begin{bmatrix} 0 & 0 & 0 & 0 \\ 0 & I & 0 & 0 \\ 0 & 0 & I & 0 \\ 0 & 0 & 0 & I \end{bmatrix} \begin{Bmatrix} d_B \\ \Theta_{x\,ij} \\ \Theta_{y\,ij} \\ W_{ij} \end{Bmatrix} \tag{52}$$

where

$$\begin{aligned}
&d_B = \begin{bmatrix} \Theta_{x_B} & \Theta_{y_B} & W_B \end{bmatrix}^{\mathrm{T}} \\
&\Theta_{x_B} = \begin{bmatrix} \Theta_{x\,11} & \Theta_{x\,1N} & \Theta_{x\,N1} & \Theta_{x\,NN} & \Theta_{x\,1j} & \Theta_{x\,i1} & \Theta_{x\,Nj} & \Theta_{x\,iN} \end{bmatrix}^{\mathrm{T}} \\
&\Theta_{y_B} = \begin{bmatrix} \Theta_{y\,11} & \Theta_{y\,1N} & \Theta_{y\,N1} & \Theta_{y\,NN} & \Theta_{y\,1j} & \Theta_{y\,i1} & \Theta_{y\,Nj} & \Theta_{y\,iN} \end{bmatrix}^{\mathrm{T}} \\
&W_B = \begin{bmatrix} W_{11} & W_{1N} & W_{N1} & W_{NN} & W_{1j} & W_{i1} & W_{Nj} & W_{iN} \end{bmatrix}^{\mathrm{T}} \\
&i, j = 2, 3, \ldots, N-2, N-1
\end{aligned}$$

and in which BB, BD, DB, DD, and I matrices are obtained according to governing and boundary equations and summarized in Appendix A.

so

$$\Omega_i = \text{Eigenvalue}\left[-\,[\mathrm{DB}]\left[[\mathrm{BB}]^{-1}[\mathrm{BD}] + [\mathrm{DD}]\right]\right] \tag{53}$$

6 Numerical Results and Discussion

Using the method described above, frequency equation (53) is solved to obtain vibration frequencies of rectangular plates with any arbitrary combination of boundary constraints. In the present study, however, we only focus on eight cases which can be obtained by combining simply supported, clamped, and free as shown in Fig. (2). To illustrate the numerical results an FG plate, the material properties of ZrO_2(ceramic) and Al(metal), as given in Table (1), are used in the numerical computations.

Table 1 The material properties of ZrO_2(ceramic) and Al (metal).

Material	$\boldsymbol{E}$ (Gpa)	$\boldsymbol{\nu}$	$\boldsymbol{\rho}$ (Kg/m^3)
$\boldsymbol{Zr\,O_2}$	200	0.3	5700
$\boldsymbol{Al}$	70	0.3	2702

Table 2 Convergence of frequency parameters $\Omega = \omega\left(I_A a^4/C_{xx}\right)^{1/2}$ with increasing number of the grid points in each element

Case	$N_x \times N_y$	Mode sequence number							
		Ω_1	Ω_2	Ω_3	Ω_4	Ω_5	Ω_6	Ω_7	Ω_8
a	7×7	19.736	48.797	48.797	78.114	96.365	96.365	125.167	125.167
	8×8	19.736	49.379	49.379	78.950	98.881	98.881	128.467	128.467
	9×9	19.732	49.373	49.373	78.939	98.977	98.977	128.413	128.413
	10×10	19.732	49.302	49.302	78.842	98.969	98.969	128.376	128.376
	11×11	19.732	49.302	49.302	78.843	98.493	98.493	127.986	127.986
	12×12	19.732	49.305	49.305	78.846	98.496	98.496	127.991	127.991
	13×13	19.735	49.305	49.304	78.846	98.524	98.524	128.013	128.013
b	7×7	35.929	76.386	76.386	109.980	138.708	139.734	166.995	166.995
	8×8	35.928	73.165	73.165	107.705	146.375	147.416	175.188	175.188
	9×9	35.944	73.235	73.235	107.843	131.070	131.703	164.105	164.105
	10×10	35.944	73.247	73.247	107.908	131.440	132.084	164.507	164.507
	11×11	35.945	73.249	73.249	107.907	131.166	131.797	164.337	164.337
	12×12	35.945	73.247	73.247	107.909	131.169	131.799	164.345	164.345
	13×13	35.945	73.247	73.247	107.909	131.152	131.783	164.333	164.333
c	7×7	23.603	51.051	58.860	85.762	97.812	117.952	130.848	141.508
	8×8	23.641	51.705	58.513	85.938	100.456	116.554	133.699	143.567
	9×9	23.632	51.680	58.653	86.087	100.514	113.069	133.856	140.497
	10×10	23.632	51.620	58.571	85.972	100.527	113.445	133.773	140.828
	11×11	23.633	51.619	58.567	85.979	100.052	112.973	133.424	140.441
	12×12	23.633	51.621	58.570	85.981	100.058	112.933	133.422	140.422
	13×13	23.633	51.622	58.570	86.981	100.085	112.957	133.446	140.440
d	7×7	31.758	63.469	74.176	101.773	120.726	137.826	152.180	161.839
	8×8	31.793	63.145	70.898	100.396	119.509	145.625	154.193	170.110
	9×9	31.794	63.308	70.924	100.562	116.158	129.849	151.316	158.763
	10×10	31.796	63.231	70.945	100.531	116.527	130.249	151.725	159.038
	11×11	31.795	63.229	70.943	100.540	116.072	129.954	151.361	158.890
	12×12	31.795	63.231	70.942	100.539	116.034	129.959	151.351	158.885
	13×13	31.795	63.237	70.942	100.540	116.058	129.941	151.366	158.875

The eigenvalues are expressed in terms of the frequency parameter as $\Omega = \omega\left(I_A a^4/C_{xx}\right)^{1/2}$. Convergence studies are carried out for the mentioned cases (a-h) to establish appropriate number of grid points for obtaining the accurate solutions. The convergence patterns of the frequency parameters with the number of grid points in each element are presented in Tables (2) and (3) for cases a–d and e–h in the same set of parameter values $\lambda_1 = 1,\ \lambda_2 = 100$ and $n = 5$. It can also be observed that the convergence rate varies for different configurations of plate.

Table 3 Convergence of frequency parameters $\Omega = \omega \left(I_A a^4/C_{xx}\right)^{1/2}$ with increasing number of the grid points in each element

Case	$N_x \times N_y$	Mode sequence number							
		Ω_1	Ω_2	Ω_3	Ω_4	Ω_5	Ω_6	Ω_7	Ω_8
e	7×7	28.918	54.185	72.626	95.371	99.819	136.821	137.168	157.347
	8×8	28.919	54.712	69.145	94.358	102.298	140.119	144.548	166.040
	9×9	28.926	54.737	69.191	94.379	102.448	128.624	140.056	154.086
	10×10	28.926	54.672	69.203	94.371	102.440	129.007	140.120	154.418
	11×11	28.926	54.673	69.203	94.371	101.983	128.712	139.759	154.235
	12×12	28.926	54.675	69.201	94.372	101.987	128.714	139.768	154.238
	13×13	28.926	54.675	69.201	94.372	102.014	128.697	139.788	154.224
f	7×7	26.972	60.618	60.935	92.842	118.953	119.273	146.090	146.916
	8×8	27.049	60.407	60.657	92.460	117.860	117.983	148.105	148.535
	9×9	27.032	60.527	60.774	92.760	114.361	114.515	145.398	145.702
	10×10	27.035	60.455	60.704	92.626	114.754	114.910	145.676	145.976
	11×11	27.035	60.449	60.698	92.641	114.286	114.436	145.326	145.630
	12×12	27.035	60.452	60.701	92.640	114.250	114.398	145.302	145.606
	13×13	27.035	60.452	60.701	92.641	114.273	114.422	145.321	145.624
g	7×7	12.016	27.928	38.338	58.251	58.715	66.409	89.707	90.443
	8×8	11.789	28.001	43.669	57.802	61.875	79.011	92.820	97.911
	9×9	11.702	27.956	42.177	60.389	60.974	95.742	104.280	108.674
	10×10	11.686	27.790	41.250	59.303	63.223	95.144	96.339	109.333
	11×11	11.683	27.752	41.187	59.110	62.053	89.799	94.784	108.706
	12×12	11.683	27.747	41.184	59.047	61.748	89.994	94.395	108.694
	13×13	11.683	27.746	41.173	59.021	61.793	90.250	94.370	108.841
h	7×7	26.205	42.182	64.354	82.799	86.006	95.991	123.188	124.935
	8×8	25.348	41.060	68.204	72.705	86.322	117.071	120.950	135.215
	9×9	24.802	41.324	65.653	73.381	84.274	117.803	120.204	133.514
	10×10	24.497	40.644	64.563	79.483	82.166	118.021	121.198	127.063
	11×11	24.309	40.455	64.055	77.719	81.651	118.165	123.285	141.836
	12×12	24.173	40.286	63.851	76.807	81.241	117.314	123.112	138.267
	13×13	24.091	40.214	63.614	76.779	81.022	117.000	122.944	133.468

In Figs. (3) - (4) for cases (a-h) and $\lambda_1 = 1$, $\lambda_2 = 100$ and $n = 1$ convergence of the first four normalized dimensionless natural frequencies Ω/Ω^* have been shown. It is observed that Ω/Ω^* converges with the increasing number of grid points in all boundary conditions. The figures related to cases a-h show that the increase of the grid points improves the convergence of the presented DQ method. For cases a-f, 13 and for g-h, 21 grid points are adequate to guarantee the convergence.

Frequency parameters corresponding to the first eight modes of vibration for cases a–f are presented in Tables (4–11). Here, aspect ratio $\left(\frac{a}{b}\right)$ of rectangular plate increases from 0.5 to 4. It can be seen that when volume fraction index n increases, there is a significant increase on natural frequency with increasing λ_1.

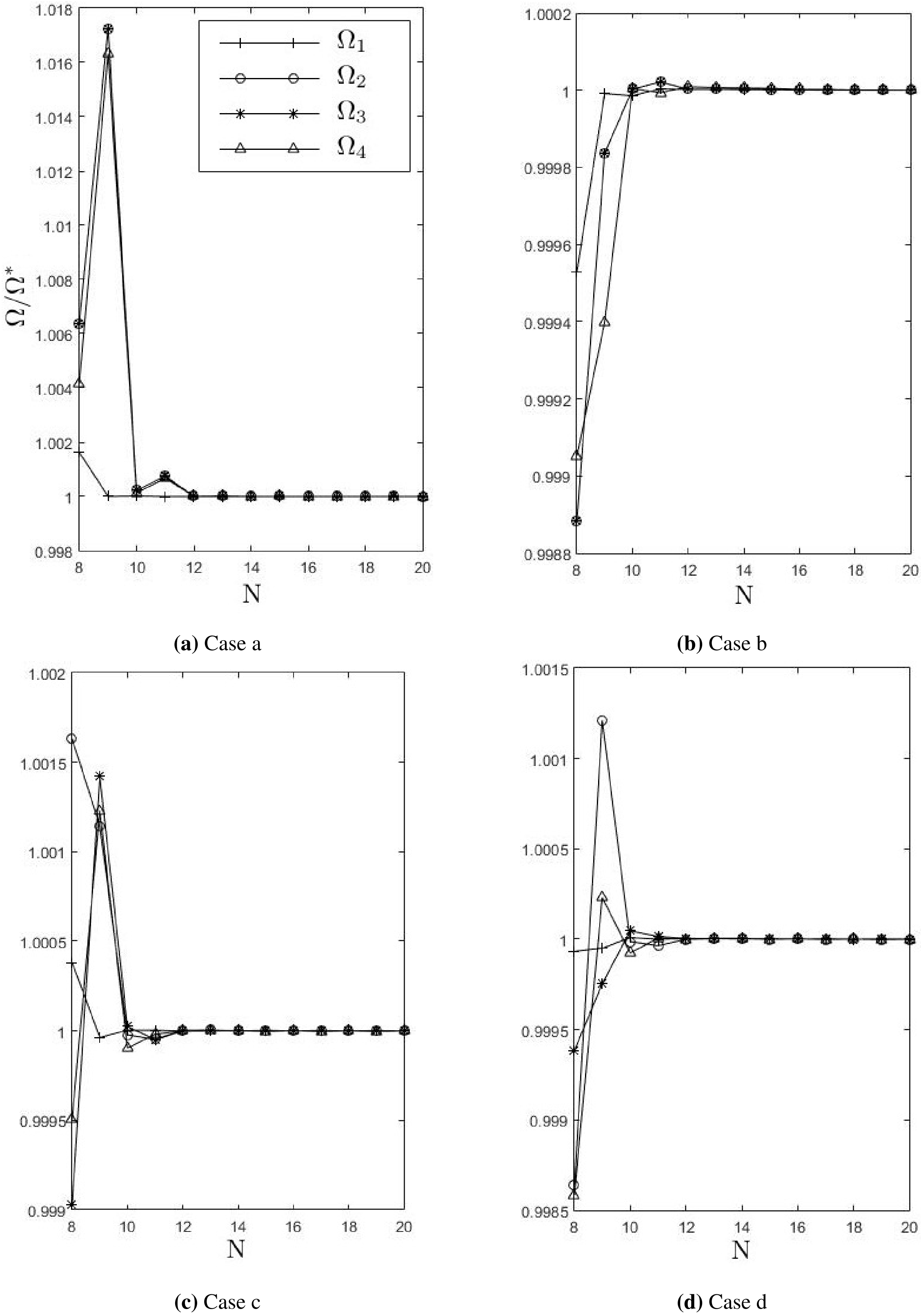

(a) Case a

(b) Case b

(c) Case c

(d) Case d

Figure 3 Convergence of normalized natural frequencies Ω/Ω^* with respect of grid points N, for $\lambda_1 = 1$, $\lambda_2 = 100$, $n = 1$ (Ω^* is DQ results using $N = 20$).

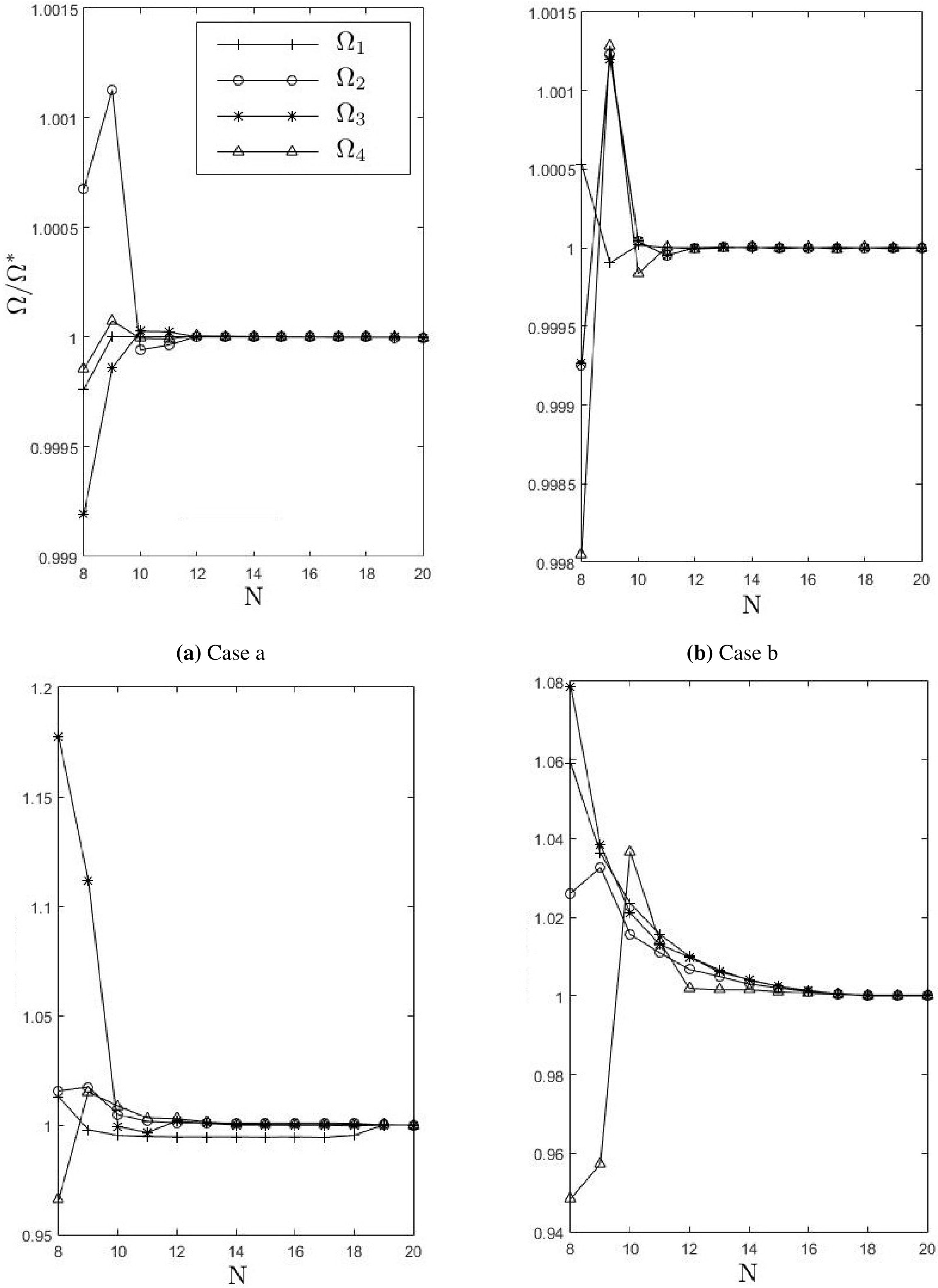

(a) Case a

(b) Case b

(c) Case c

(d) Case d

Figure 4 Convergence of normalized natural frequencies Ω/Ω^* with respect of grid points N, for $\lambda_1 = 1$, $\lambda_2 = 100$, $n = 1$ (Ω^* is DQ results using $N = 20$).

Table 4 Convergence of frequency parameters $\Omega = \omega \left(I_A a^4/C_{xx}\right)^{1/2}$ with increasing λ_1 for a simply supported rectangular plate (SSSS)

λ_1	References	Mode sequence number of case a							
		Ω_1	Ω_2	Ω_3	Ω_4	Ω_5	Ω_6	Ω_7	Ω_8
0.4	Leissa [3]	11.449	16.182	24.082	35.136	41.058	45.795	49.348	53.691
	Present	11.446	16.181	24.071	35.097	41.026	45.756	49.235	53.637
0.5	Liew et al. [21]	12.34	19.74	32.08	41.95	49.35	49.35	61.69	71.55
	Present	12.334	19.732	32.057	41.913	49.275	49.303	61.614	71.351
2/3	Leissa [3]	14.256	27.416	43.865	49.348	58.024	78.957	80.053	93.213
	Present	14.252	27.402	43.829	49.303	56.964	78.841	79.882	93.053
1	Liew et al. [21]	19.74	49.35	49.35	78.96	98.70	98.70	128.3	128.3
	Dawe [22]	19.732	49.303	49.303	78.841	98.515	98.515	127.999	127.999
	Eftekhari [17]	19.739	49.348	49.348	78.957	98.696	98.696	128.305	128.305
	Liu [23]	19.732	49.303	49.303	78.841	98.515	98.515	127.999	127.999
	Leissa [3]	19.739	49.348	49.348	78.957	98.696	98.696	128.305	128.305
	Present	19.732	49.303	49.303	78.841	98.516	98.516	128.000	128.000
1.5	Leissa [3]	32.076	61.685	98.696	111.330	128.305	177.653	180.120	209.729
	Present	32.057	61.614	98.515	110.805	127.999	177.069	179.404	208.918
2	Liew et al. [3]	49.35	78.96	128.3	167.8	197.4	197.4	246.7	286.2
	Present	49.303	78.841	128.000	167.262	196.564	196.671	245.616	284.278
2.5	Leissa[3]	71.556	101.163	150.511	219.599	256.610	286.218	308.425	335.566
	Present	71.459	100.973	150.092	218.609	255.393	284.707	306.255	333.492
4	Liew et al. [21]	167.8	197.4	246.7	315.8	404.7	513.2	641.5	641.5
	Present	167.261	196.671	245.615	313.915	401.267	518.784	634.018	650.344

Table 5 Convergence of frequency parameters $\Omega = \omega \left(I_A a^4/C_{xx}\right)^{1/2}$ with increasing λ_1 for a clamped rectangular plate (CCCC)

λ_1	References	Mode sequence number of case b							
		Ω_1	Ω_2	Ω_3	Ω_4	Ω_5	Ω_6	Ω_7	Ω_8
0.4	Leissa [3]	23.648	27.817	35.446	46.702	61.554	63.100	—	—
	Present	23.624	27.781	35.378	46.621	61.425	62.969	67.260	74.621
0.5	Liew et al. [21]	25.58	31.83	44.77	63.33	63.98	71.08	83.27	87.25
	Present	24.557	31.793	44.711	63.246	63.866	70.932	83.081	87.121
2/3	Leissa [3]	27.010	41.716	66.143	66.552	79.850	100.85	—	—
	Present	26.980	41.650	65.999	66.401	79.625	100.600	102.838	124.891
1	Liu [23]	35.937	73.232	73.232	107.889	131.118	131.752	164.300	164.300
	C.H.W. Ng [24]	35.989	73.407	73.407	108.249	131.622	132.244	165.074	165.074
	Eftekhari [17]	35.985	73.394	73.394	108.217	131.581	132.206	—	—
	Leissa [3]	35.992	73.413	73.413	108.27	131.64	132.24	—	—
	Present	35.942	73.237	73.237	107.888	131.125	131.756	164.291	164.291
1.5	Leissa [3]	60.772	93.860	148.82	149.74	179.66	226.92	—	—
	Present	60.636	93.565	148.148	149.068	178.658	225.642	230.594	279.884
2	Liew et al. [21]	98.31	127.3	179.1	253.3	256.0	284.3	333.1	349.0
	Present	97.981	126.784	178.158	251.737	254.077	282.040	330.076	346.283
2.5	Leissa [3]	147.80	173.85	221.54	291.89	384.71	394.37	—	—
	Present	147.029	172.795	219.870	289.423	380.780	389.892	416.233	461.384
4	Liew et al. [21]	364.8	386.3	425.1	484.0	564.7	668.0	793.8	941.6
	Present	360.292	381.270	419.182	476.718	555.501	669.288	793.613	967.856

Table 6 Convergence of frequency parameters $\Omega = \omega \left(I_A a^4/C_{xx}\right)^{1/2}$ with increasing λ_1 for one edge clamped and the other edges simply supported rectangular plate (SCSS)

λ_1	References	Mode sequence number of case c							
		Ω_1	Ω_2	Ω_3	Ω_4	Ω_5	Ω_6	Ω_7	Ω_8
0.4	Leissa [3]	11.750	17.187	25.917	37.832	41.207	46.362	52.901	54.872
	Present	11.747	17.181	25.903	37.790	41.175	46.321	52.858	54.811
0.5	Liew et al. [21]	12.92	21.53	35.21	42.24	50.43	53.82	63.87	77.35
	Present	12.915	21.523	35.184	42.206	50.382	53.742	63.784	77.260
2/3	Leissa [3]	15.573	31.072	44.564	55.393	59.463	83.606	88.438	93.676
	Present	15.573	31.050	44.526	55.325	59.391	83.460	88.233	93.512
1	Liew et al. [21]	23.65	51.67	58.65	86.13	100.3	113.2	133.8	140.9
	C.H.W. Ng [24]	23.647	51.675	58.650	86.141	100.272	113.241	133.801	140.864
	Liu [23]	23.632	51.619	58.565	85.972	100.075	112.944	113.427	140.419
	Leissa [3]	23.646	51.673	58.646	86.134	100.270	113.228	133.791	140.846
	Present	23.632	51.619	58.565	85.972	100.077	112.942	133.429	140.418
1.5	Leissa [3]	42.528	69.003	116.267	120.996	147.635	184.101	193.802	243.496
	Present	42.478	68.892	115.989	120.646	147.134	183.325	192.987	242.178
2	Liew et al. [21]	69.33	94.59	140.2	206.7	208.4	234.6	279.7	293.8
	Present	69.193	94.359	139.766	205.714	207.355	233.298	277.887	291.640
2.5	Leissa [3]	103.923	128.338	172.380	237.250	322.964	346.738	391.066	429.242
	Present	103.618	127.903	171.670	235.929	318.342	320.423	343.911	387.556
4	Liew et al. [21]	255.9	284.3	333.1	403.2	494.7	607.6	741.4	808.9
	Present	252.315	275.181	315.422	374.716	453.865	563.594	688.985	792.657

Table 7 Convergence of frequency parameters $\Omega = \omega \left(I_A a^4/C_{xx}\right)^{1/2}$ with increasing λ_1 for one edge simply supported and the other edges clamped rectangular plate (CSCC)

λ_1	References	Mode sequence number of case d							
		Ω_1	Ω_2	Ω_3	Ω_4	Ω_5	Ω_6	Ω_7	Ω_8
0.4	Leissa [3]	23.440	27.022	33.799	44.131	58.034	62.971	—	—
	Present	23.420	26.991	33.750	44.046	57.928	62.851	66.798	73.611
0.5	Present	24.123	30.220	41.701	58.748	63.625	70.003	81.110	81.243
2/3	Leissa [3]	25.861	38.102	60.325	65.516	77.563	92.154	—	—
	Present	25.837	38.051	60.211	65.387	77.368	91.883	98.341	124.477
1	C.H.W. Ng [24]	31.828	63.338	71.087	100.815	116.376	130.388	151.938	159.534
	Eftekhari [17]	31.826	63.331	71.076	100.792	116.357	130.353	—	—
	Leissa [3]	31.829	63.347	71.084	100.83	116.40	130.37	—	—
	Present	31.793	63.225	70.933	100.524	116.041	129.915	151.335	158.839
1.5	Leissa [3]	48.167	85.507	123.99	143.99	158.36	214.78	—	—
	Present	48.089	85.287	123.570	143.417	157.638	213.389	221.483	244.120
2	Present	73.237	107.889	164.292	209.450	240.748	241.764	294.212	338.115
2.5	Leissa [3]	107.07	139.66	194.41	270.48	322.55	353.43	—	—
	Present	106.714	139.064	193.264	268.605	319.954	350.156	364.198	400.872
4	Present	254.077	282.040	330.076	398.986	488.760	613.448	745.957	793.589

Table 8 Convergence of frequency parameters $\Omega = \omega \left(I_A a^4 / C_{xx}\right)^{1/2}$ with increasing λ_1 for one pair of opposite sides which are clamped and the other opposite sides which are simply supported in the considered rectangular plate (SCSC)

λ_1	References	Mode sequence number of case e							
		Ω_1	Ω_2	Ω_3	Ω_4	Ω_5	Ω_6	Ω_7	Ω_8
0.4	Leissa [3]	12.135	18.365	27.966	40.750	41.378	47.001	56.178	56.676
	Present	12.131	18.357	27.947	40.724	41.346	46.956	56.113	56.635
0.5	Liew et al. [21]	13.69	23.65	38.69	42.59	51.67	58.65	66.30	83.49
	Present	13.681	23.632	38.657	42.551	51.618	58.588	66.204	83.388
2/3	Leissa [3]	17.373	35.344	45.429	62.054	62.313	88.805	94.213	97.425
	Present	17.365	35.311	45.387	61.958	62.226	88.624	94.045	97.245
1	Liew et al. [21]	28.95	54.74	69.33	94.59	102.2	129.1	140.2	154.8
	Liu [24]	28.922	54.666	69.193	94.359	101.994	128.674	139.765	154.199
	C.H.W. Ng [24]	28.953	54.747	69.337	94.601	102.222	129.130	140.230	154.823
	Eftekhari [17]	28.951	54.743	69.327	94.585	102.216	129.095	140.204	154.776
	Leissa [3]	28.951	54.743	69.327	94.585	102.216	129.095	140.204	154.776
	Present	28.924	54.671	69.193	94.359	102.004	128.672	139.765	154.191
1.5	Leissa [3]	56.348	78.983	123.172	146.268	170.111	189.122	212.817	276.001
	Present	56.240	78.801	122.812	145.663	169.326	188.259	211.681	274.063
2	Liew et al. [21]	95.26	115.8	156.4	219.0	254.1	277.3	303.4	318.1
	Present	94.951	115.372	155.686	217.740	252.315	275.181	300.986	315.421
2.5	Leissa [3]	145.484	164.739	202.227	261.105	342.144	392.875	415.691	455.305
	Present	144.759	163.834	200.993	259.219	339.008	388.539	410.895	449.702
4	Liew et al. [21]	363.5	381.1	413.3	463.2	533.5	625.4	739.6	875.9
	Present	359.031	376.153	407.614	456.428	524.879	623.784	740.338	967.080

Table 9 Convergence of frequency parameters $\Omega = \omega \left(I_A a^4 / C_{xx}\right)^{1/2}$ with increasing λ_1 for two attached clamped edges and two attached simply supported edges in the analyzed rectangular plate (CSSC)

λ_1	References	Mode sequence number of case f							
		Ω_1	Ω_2	Ω_3	Ω_4	Ω_5	Ω_6	Ω_7	Ω_8
0.4	Leissa [3]	16.849	21.363	29.236	40.509	51.457	55.117	—	—
	Present	16.839	21.345	29.204	40.444	51.386	55.040	55.888	63.513
0.5	Present	17.760	25.181	37.938	52.276	55.898	59.501	71.759	79.012
2/3	Leissa [3]	19.952	34.024	54.370	57.517	67.815	90.069	—	—
	Present	19.940	33.990	54.292	57.430	67.680	89.835	90.293	108.362
1	C.H.W. Ng [24]	27.055	60.543	60.791	92.849	114.572	114.719	145.811	146.109
	Eftekhari [17]	27.054	60.534	60.786	92.836	114.556	114.704	—	—
	Leissa [3]	27.056	60.544	60.791	92.865	114.57	114.72	—	—
	Present	27.033	60.447	60.696	92.630	114.257	114.406	145.295	145.599
1.5	Leissa [3]	44.893	76.554	122.33	129.41	152.58	202.66	—	—
	Present	44.833	76.395	121.956	129.002	151.971	201.630	202.634	243.077
2	Present	70.933	100.524	151.336	208.316	222.752	236.990	285.597	314.432
2.5	Leissa [3]	105.31	133.52	182.73	253.18	321.60	344.48	—	—
	Present	104.982	133.001	181.823	251.531	319.096	341.808	346.869	393.867
4	Present	253.127	278.377	322.330	386.284	470.788	587.181	718.921	793.100

Table 10 Convergence of frequency parameters $\Omega = \omega\left(I_A a^4/C_{xx}\right)^{1/2}$ with increasing λ_1 for one edge free and the other edges simply supported rectangular plate (SSSF)

λ_1	References	Mode sequence number of case g							
		Ω_1	Ω_2	Ω_3	Ω_4	Ω_5	Ω_6	Ω_7	Ω_8
0.4	Leissa [3]	10.126	13.057	18.839	27.558	39.338	39.612	42.696	48.774
	Present	8.736	12.107	17.673	26.378	34.882	38.230	41.449	46.975
0.5	Present	9.227	13.707	22.409	35.973	36.607	42.992	51.851	54.443
2/3	Leissa [3]	10.671	18.299	33.697	40.131	48.408	57.593	64.728	89.156
	Present	9.963	17.329	32.681	38.464	46.909	56.671	62.778	86.134
1	Eftekhari [17]	11.684	27.756	41.197	59.065	61.861	90.294	94.484	108.918
	Leissa [3]	11.684	27.756	41.197	59.065	61.861	90.294	94.484	108.918
	Present	11.682	27.745	41.168	59.008	61.800	90.152	94.337	108.714
1.5	Leissa [3]	13.711	43.572	47.857	81.479	92.693	124.563	132.897	158.918
	Present	15.399	45.935	50.518	86.335	95.672	126.383	138.411	164.236
2	Present	20.511	52.443	81.356	102.758	123.715	172.429	179.794	215.721
2.5	Leissa [3]	18.801	50.540	100.232	110.226	147.632	169.103	203.730	257.479
	Present	26.853	60.881	111.813	120.022	170.381	181.870	232.275	271.225
4	Present	51.785	97.440	151.868	223.093	282.096	313.149	361.593	422.311

Table 11 Convergence of frequency parameters $\Omega = \omega\left(I_A a^4/C_{xx}\right)^{1/2}$ with increasing λ_1 for one edge free and the other edges clamped rectangular plate (CCCF)

λ_1	References	Mode sequence number of case h							
		Ω_1	Ω_2	Ω_3	Ω_4	Ω_5	Ω_6	Ω_7	Ω_8
0.4	Leissa [3]	22.577	24.623	29.244	37.059	48.283	61.922	—	—
	Present	21.689	24.709	28.548	36.122	47.614	61.559	62.636	63.987
0.5	Present	21.828	25.536	33.183	45.740	61.321	64.211	65.150	73.074
2/3	Leissa [3]	23.015	29.427	44.363	62.417	68.887	69.696	—	—
	Present	22.711	28.781	43.594	61.981	68.029	68.872	83.646	101.959
1	Leissa [3]	24.020	40.039	63.493	76.761	80.713	116.80	—	—
	Present	24.163	40.271	63.788	76.826	81.107	117.042	123.102	134.268
1.5	Leissa [3]	26.731	65.916	66.219	106.80	125.40	152.48	—	—
	Present	28.895	68.876	69.061	112.594	128.674	154.391	173.736	197.084
2	Present	36.511	77.293	109.748	136.933	158.501	216.167	222.339	263.162
2.5	Leissa [3]	37.656	76.407	135.15	152.47	193.01	213.74	—	—
	Present	46.967	89.122	148.365	162.144	217.634	227.352	286.430	325.673
4	Present	93.507	147.186	207.431	283.868	379.180	386.142	467.619	509.119

In tables (12–19), the numerical results of frequency parameters corresponding to the first eight modes (a–h) of vibration of square plate with different a/h has been reported. In these tables, it is evident that the frequency parameters for each case increase gradually as the λ_2 ratio decreases from 100 to 5. It can also be seen that λ_2 is more effective in higher modes with respect to first modes of vibration.

Table 12 Convergence of frequency parameters $\Omega = \omega\left(I_A a^4/C_{xx}\right)^{1/2}$ with increasing λ_2 for a simply supported (SSSS)

λ_2	References	Mode sequence number of case a							
		Ω_1	Ω_2	Ω_3	Ω_4	Ω_5	Ω_6	Ω_7	Ω_8
100	Dawe [22]	19.731	49.303	49.303	78.840	98.514	98.514	——	——
	Leissa [3]	19.739	49.348	49.348	78.957	98.696	98.696	128.305	128.305
	Present	19.732	49.303	49.303	78.841	98.516	98.516	128.000	128.000
10	Liu [23]	19.058	45.448	45.448	69.717	84.926	84.926	106.515	106.515
	Present	19.058	45.448	45.448	69.717	84.927	84.927	106.516	106.516
5	Liew et al. [21]	17.448	38.152	38.152	55.150	65.145	65.145	——	——
	Liu [23]	17.429	38.073	38.073	55.002	64.951	64.951	78.434	78.434
	Present	17.429	38.073	38.073	55.002	64.952	64.952	78.434	78.434

Table 13 Convergence of frequency parameters $\Omega = \omega\left(I_A a^4/C_{xx}\right)^{1/2}$ with increasing λ_2 for a clamped (CCCC)

λ_2	References	Mode sequence number of case b							
		Ω_1	Ω_2	Ω_3	Ω_4	Ω_5	Ω_6	Ω_7	Ω_8
100	Liew et al. [21]	35.99	73.40	73.40	108.2	131.6	132.2	165.0	165.0
	Liu [23]	35.937	73.232	73.232	107.889	131.119	131.752	164.300	164.300
	Present	35.942	73.237	73.237	107.888	131.125	131.756	164.291	164.291
10	Liu [23]	32.489	61.937	61.937	86.778	102.207	103.185	123.595	123.595
	Present	32.489	61.937	61.937	86.777	102.207	103.185	123.595	123.595
5	Liu [23]	26.453	46.135	46.135	61.930	70.549	71.521	83.697	83.697
	Present	26.453	46.135	46.135	61.930	70.549	71.521	83.697	83.697

Table 14 Convergence of frequency parameters $\Omega = \omega\left(I_A a^4/C_{xx}\right)^{1/2}$ with increasing λ_2 for one edge clamped and the other edges simply supported (SCSS)

λ_2	References	Mode sequence number of case c							
		Ω_1	Ω_2	Ω_3	Ω_4	Ω_5	Ω_6	Ω_7	Ω_8
100	Liew et al. [21]	23.65	51.67	58.65	86.13	100.3	113.2	133.8	140.9
	Liu [23]	23.632	51.619	58.565	85.972	100.075	112.943	133.427	140.419
	Present	23.632	51.619	58.565	85.972	100.077	112.942	133.429	140.418
10	Liu [23]	22.376	47.063	52.090	74.004	85.759	93.064	109.072	112.527
	Present	22.376	47.063	52.090	74.004	85.760	93.066	109.073	112.527
5	Liu [23]	19.671	38.860	41.334	56.667	65.248	67.699	79.210	80.160
	Present	19.671	38.860	41.334	56.667	65.248	67.700	79.210	80.160

Table 15 Convergence of frequency parameters $\Omega = \omega\left(I_A a^4/C_{xx}\right)^{1/2}$ with increasing λ_2 for one edge simply supported and the other edges clamped (CSCC)

λ_2	References	Mode sequence number of case d							
		Ω_1	Ω_2	Ω_3	Ω_4	Ω_5	Ω_6	Ω_7	Ω_8
100	Present	31.793	63.225	70.933	100.523	116.041	129.915	151.335	158.839
10		29.103	55.262	60.361	82.519	94.707	101.869	117.646	121.014
5		24.146	43.009	45.230	60.129	68.359	70.666	81.884	82.761

Table 16 Convergence of frequency parameters $\Omega = \omega\left(I_A a^4/C_{xx}\right)^{1/2}$ with increasing λ_2 for one pair of opposite sides which are clamped and the other opposite sides which are simply supported in the considered (SCSC)

λ_2	References	Mode sequence number of case e							
		Ω_1	Ω_2	Ω_3	Ω_4	Ω_5	Ω_6	Ω_7	Ω_8
100	Liu [23]	28.922	54.666	69.193	94.359	101.994	128.674	139.765	154.199
	Present	28.924	54.671	69.193	94.359	102.004	128.672	139.765	154.191
10	Liu [23]	32.489	61.937	61.937	86.778	102.207	103.185	123.595	123.595
	Present	26.645	49.062	59.118	78.683	86.721	101.152	111.848	118.657
5	Liu [23]	22.308	39.756	44.467	58.357	65.567	70.285	80.006	81.840
	Present	22.308	39.756	44.467	58.357	65.568	70.284	80.006	81.840

Table 17 Convergence of frequency parameters $\Omega = \omega\left(I_A a^4/C_{xx}\right)^{1/2}$ with increasing λ_2 for two attached clamped edges and two attached simply supported edges in the analyzed (CSSC)

λ_2	References	Mode sequence number of case f							
		Ω_1	Ω_2	Ω_3	Ω_4	Ω_5	Ω_6	Ω_7	Ω_8
100	Leissa [3]	27.056	60.544	60.791	92.865	114.57	114.72	——	——
	C.H.W. Ng [24]	27.055	60.543	60.791	92.849	114.572	114.719	145.811	146.109
	Present	27.033	60.447	60.696	92.630	114.257	114.406	145.295	145.599
10		25.265	53.328	53.667	78.054	93.710	93.948	114.747	115.202
5		21.694	41.917	42.299	58.380	67.905	68.154	80.852	81.171

Table 18 Convergence of frequency parameters $\Omega = \omega\left(I_A a^4/C_{xx}\right)^{1/2}$ with increasing λ_2 for one edge free and the other edges simply supported (SSSF)

λ_2	References	Mode sequence number of case g							
		Ω_1	Ω_2	Ω_3	Ω_4	Ω_5	Ω_6	Ω_7	Ω_8
100	Leissa [3]	11.684	27.756	41.197	59.065	61.861	90.294	94.484	108.918
	Eftekhari [17]	11.684	27.756	41.197	59.065	61.861	90.294	94.484	108.918
	Present	11.682	27.745	41.168	59.008	61.800	90.152	94.337	108.714
10		11.488	26.706	38.656	54.196	56.711	79.147	83.017	93.502

Table 19 Convergence of frequency parameters $\Omega = \omega \left(I_A a^4/C_{xx}\right)^{1/2}$ with increasing λ_2 for one edge free and the other edges clamped (CCCF)

λ_2	References	Mode sequence number of case h							
		Ω_1	Ω_2	Ω_3	Ω_4	Ω_5	Ω_6	Ω_7	Ω_8
100	Leissa [3]	24.020	40.039	63.493	76.761	80.713	116.80	—	—
	Present	23.918	39.994	63.185	76.649	80.516	116.514	122.064	134.175
10		24.056	39.024	59.747	70.445	74.533	102.929	107.377	114.721

Figs. (5–13) show the variation of the first natural frequency versus n volume fraction index of FG plates for eight different boundary conditions. It can be seen how ω_1 changes with n and λ_1.

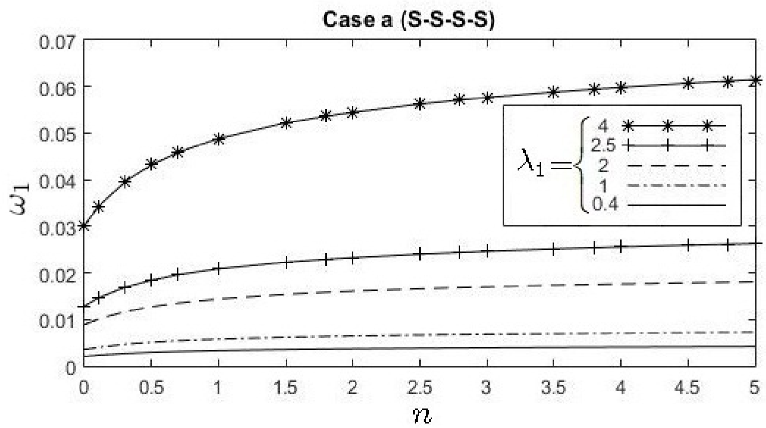

Figure 5 Effect of volume fraction index of FG plate on First natural frequency ω_1 of case a for $\lambda_1 = 0.4, 1, 2, 2.5, 4$ and $\lambda_2 = 100$

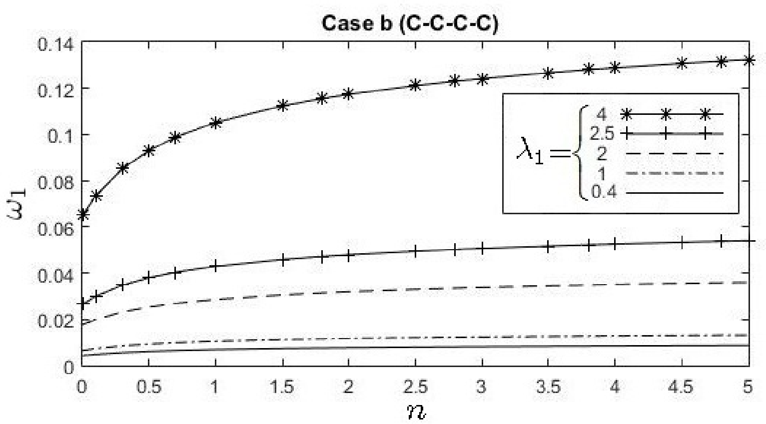

Figure 6 Effect of volume fraction index of FG plate on First natural frequency ω_1 of case b for $\lambda_1 = 0.4, 1, 2, 2.5, 4$ and $\lambda_2 = 100$

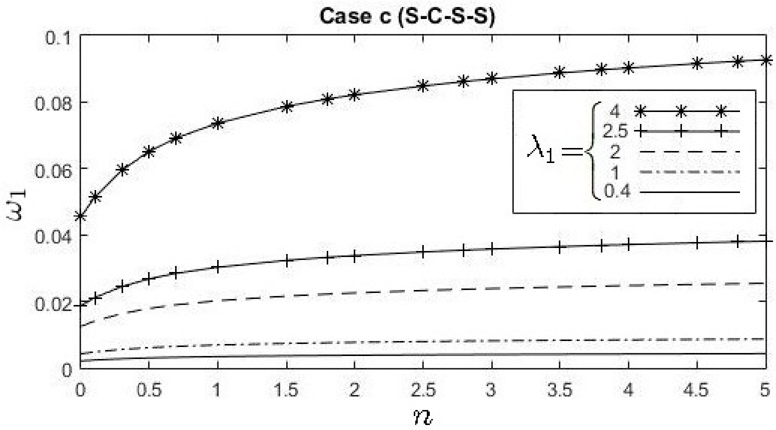

Figure 7 Effect of volume fraction index of FG plate on First natural frequency ω_1 of case c for $\lambda_1 = 0.4, 1, 2, 2.5, 4$ and $\lambda_2 = 100$

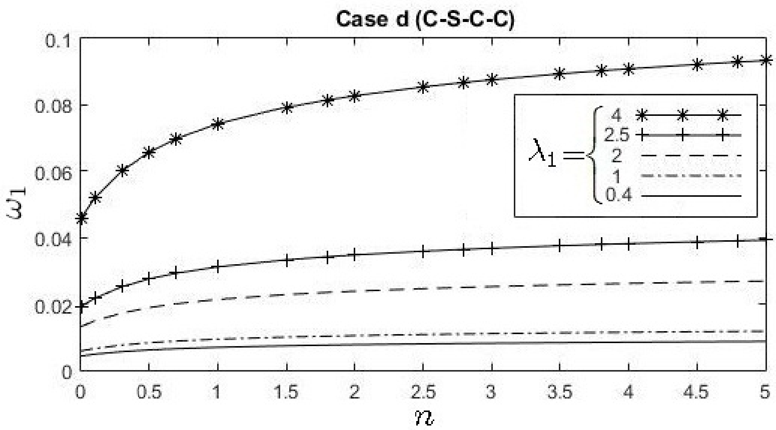

Figure 8 Effect of volume fraction index of FG plate on First natural frequency ω_1 of case d for $\lambda_1 = 0.4, 1, 2, 2.5, 4$ and $\lambda_2 = 100$

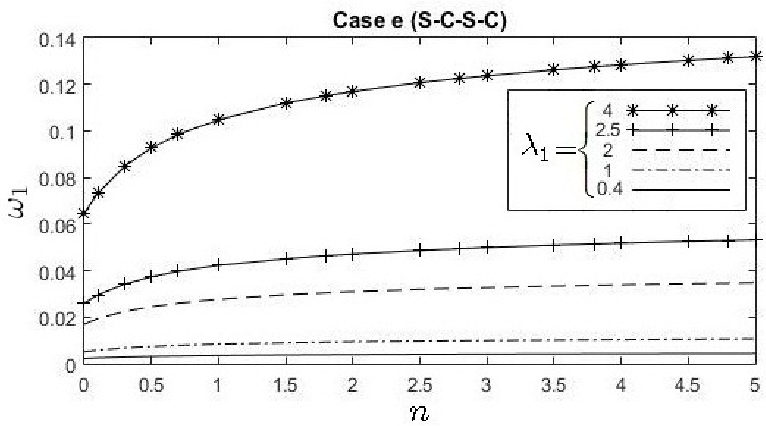

Figure 9 Effect of volume fraction index of FG plate on First natural frequency ω_1 of case e for $\lambda_1 = 0.4, 1, 2, 2.5, 4$ and $\lambda_2 = 100$

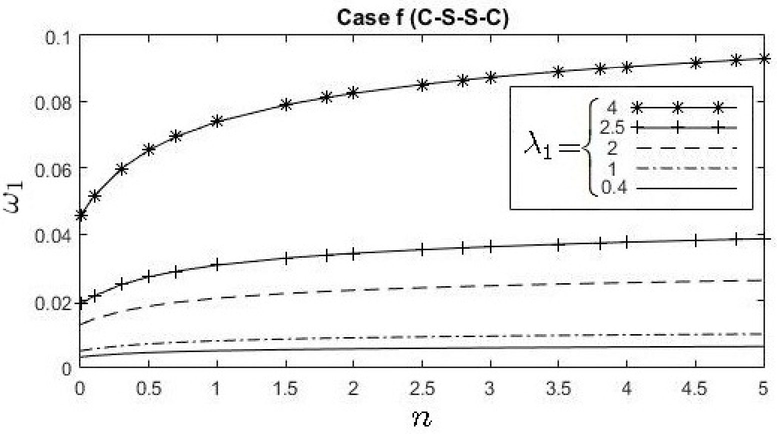

Figure 10 Effect of volume fraction index of FG plate on First natural frequency ω_1 of case f for $\lambda_1 = 0.4, 1, 2, 2.5, 4$ and $\lambda_2 = 100$

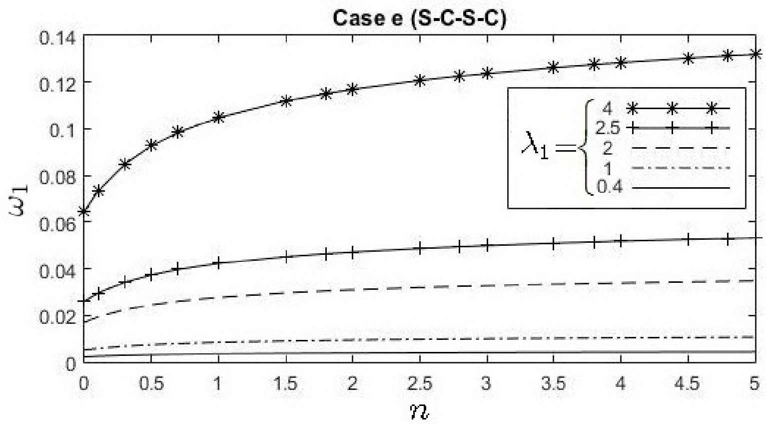

Figure 11 Effect of volume fraction index of FG plate on First natural frequency ω_1 of case f for $\lambda_1 = 0.4, 1, 2, 2.5, 4$ and $\lambda_2 = 100$

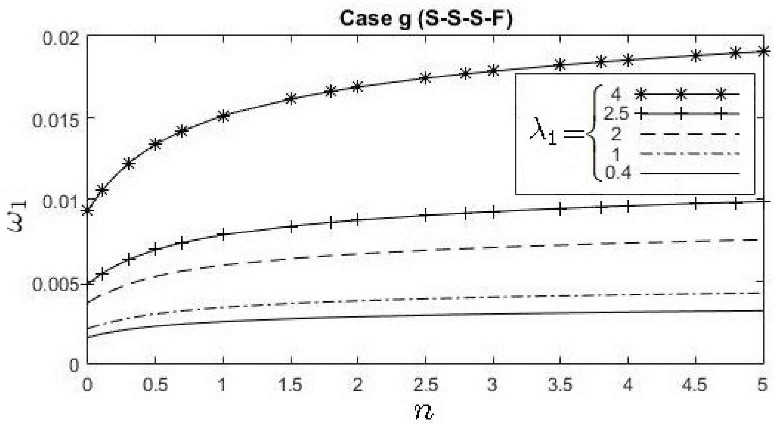

Figure 12 Effect of volume fraction index of FG plate on First natural frequency ω_1 of case g for $\lambda_1 = 0.4, 1, 2, 2.5, 4$ and $\lambda_2 = 100$

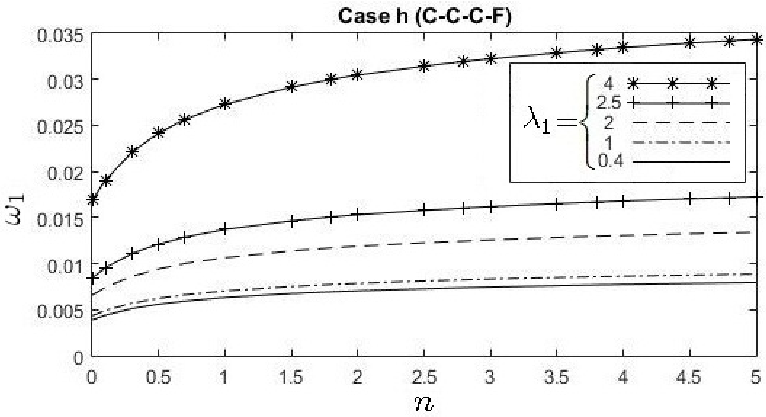

Figure 13 Effect of volume fraction index of FG plate on First natural frequency ω_1 of case h for $\lambda_1 = 0.4, 1, 2, 2.5, 4$ and $\lambda_2 = 100$

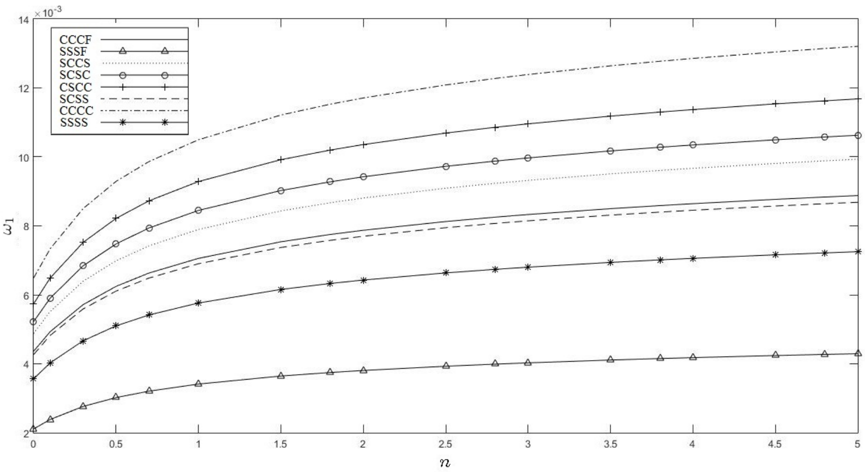

Figure 14 Effect of volume fraction index and different boundary conditions on First natural frequency ω_1 for $\lambda_1 = 1$ and $\lambda_2 = 100$

Fig. (14) shows effect of volume fraction index on natural frequency at different boundary conditions. Natural frequency is maximized when all edges are clamped and it is minimized at SSSF boundary condition for any volume fraction index.

7 Conclusions

In the present paper, free vibration analysis of functionally graded rectangular plate via two dimensional DQ method has been presented on the basis of Mindlin plate theory and for different types of boundary conditions. It is concluded that:

1. The choose of appropriate number of grid points in convergence of DQM depends on boundary condions of plate.
2. The natural frequencies of plate increase in any boundary conditions when volume fraction index increases.
3. maximum and minimum of first natural frequency of the plate are related to CCCC and SSSF boundary edges respectively.
4. First natural frequency at SCSS case is so closed to CCCF case. It seems that when λ_1 increases the effect of volume fraction index is more.

5. In square plate, Natural frequency at SCSC case is more than it in SCCS case. It seems that stiffness of plate at SCSC boundary condition is more than it at SCCS.

References

[1] Shen, H. S., and Wang, Z. X., "Assessment of Voigt and Mori-Tanaka Models for Vibration Analysis of Functionally Graded Plates", Composite Structures, Vol. 94, pp. 2197–2208, (2012).

[2] Leissa, A.W., "Vibration of Plates", US Government Printing Office, Washington, (1969).

[3] Leissa, A.W., "The Free Vibration of Rectangular Plates", Journal of Sound and Vibration, Vol. 31, pp. 257–293, (1973).

[4] Gorman, D ., "Exact Solutions for the Free In-plane Vibration of Rectangular Plates with Two Opposite Edges Simply Supported", Journal of Sound and Vibration, Vol. 294, pp. 131–61, (2006).

[5] Matsunaga, H., "Vibration and Stability of Thick Plates on Elastic Foundations", Journal of Engineering Mechanics ,Vol. 126, pp. 27–34, (2000).

[6] Li, R., Tian, Y., Wang, P., Shi, Y. and Wang, B., "New Analytic Free Vibration Solutions of Rectangular Thin Plates Resting on Multiple Point Supports", International Journal of Mechanical Sciences, Vol. 110, pp. 53–61, (2016).

[7] Fallah, A., Aghdam, M. M., and Kargarnovin, M. H., "Free Vibration Analysis of Moderately Thick Functionally Graded Plates on Elastic Foundation using the Extended Kantorovich Method", Archive of Applied Mechanics, Vol. 83, pp. 177–191, (2013).

[8] Xing, Y. F., and Xu, T. F.,"Solution Methods of Exact Solutions for Free Vibration of Rectangular Orthotropic Thin Plates with Classical Boundary Conditions", Composite Structures, Vol. 104, pp. 187–195, (2013).

[9] Shu, C., "*Differential Quadrature and its Application in Engineering,*" Springer Publication, Washington, (1969).

[10] Tang, Y., and Wang, X., "Buckling of Symmetrically Laminated Rectangular Plates under Parabolic Edge Compression", International Journal of Mechanical Sciences,Vol. 53, pp. 91–97, (2011).

[11] Bellman, R. E., and Casti, J., "Differential Quadrature and Long Term Integrations", Journal of Mathematical Analysis and Applications, Vol. 34, pp. 235–238, (1971).

[12] Bellman, R. E., Kashef, B. G., and Casti, J., "Differential Quadrature: a Technique for the Rapid Solution of Nonlinear Partial Differential Equations", Journal of Computational Physics, Vol. 10 , pp. 40–52 ,(1972).

[13] Malekzadeh, P., and Karami, G., "Vibration of Non-uniform Thick Plates on Elastic Foundation by Differential Quadrature Method", Engineering Structures, Vol. 26, pp. 1473–1482, (2004).

[14] Ferreira, A. J. M., Carrera, E.,Cinefra, M., Viola, E., Tornabene, F., Fantuzzi, N., and Zenkour, A. M., "Analysis of Thick Isotropic and Cross-ply Laminated Plates by Generalized Differential Quadrature Method and a Unified Formulation", Composites: Part B, Vol. 58, pp. 544–552, (2014).

[15] Li, R., Wang, P., Xue, R., and Guo, X., "New Analytic Solutions for Free Vibration of Rectangular Thick Plates with an Edge Free", International Journal of Mechanical Sciences, Vol. 131-132, pp. 179-190, (2017).

[16] Malekzadeh, P., and Monajjemzadeh, S. M., "Nonlinear Response of Functionally Graded Plates under Moving Load", Thin-Walled Structures, Vol. 96, pp. 120–129, (2015).

[17] Eftekhari, S. A., and Jafari, A. A., "A Mixed Method for Free and Forced Vibration of Rectangular Plates", Applied Mathematical Modelling, Vol. 36, pp. 2814–2831, (2012).

[18] Wakashima, K., Hirano, T., and Niino, M., "Space Applications of Advanced Structural Materials", US Government Printing Office, European Space Agency, pp. 303–397, (1990).

[19] Bert, C. W., and Malik, M., "Differential Quadrature Method in Computational Mechanics: a Review", Applied Mechanics Reviews, Vol. 49, pp. 1–28, (1996).

[20] Quan, J. R., and Chang, C. T., "New Insights in Solving Distributed System Equations by the Quadrature Methods I: Analysis", Computers and Chemical Engineering, Vol. 13, pp. 779–788, (1989).

[21] Liew, K. M., Hung, K. C., and Lim, M. K., "Roles of Domain Decomposition Method in Plate Vibrations: Treatment of Mixed Discontinuous Periphery Boundaries", International Journal of Mechanical Science, Vol. 35, pp. 615–632, (1993).

[22] Dawe, D. J., "Buckling and Vibration of Plate Structures Including Shear Deformation and Related Effects", Aspects of the Analysis of Plate Structures, pp. 73–99, (1985).

[23] Liu, F. L., and Liew, K. M., "Analysis of Vibrating Thick Rectangular Plates with Mixed Boundary Constraints using Differential Quadrature Element Method", Journal of Sound and Vibration, Vol. 225, pp. 915–934, (1999).

[24] Ng, C. H. W., Zhao, Y. B., and Wei, G. W., "Comparison of Discrete Singular Convolution and Qeneralized Differential Quadrature for the Vibration Analysis of Rectangular Plates", Comput. Methods Appl. Mech. Eng., Vol. 193, pp. 2483–2506, (2004).

A Appendix

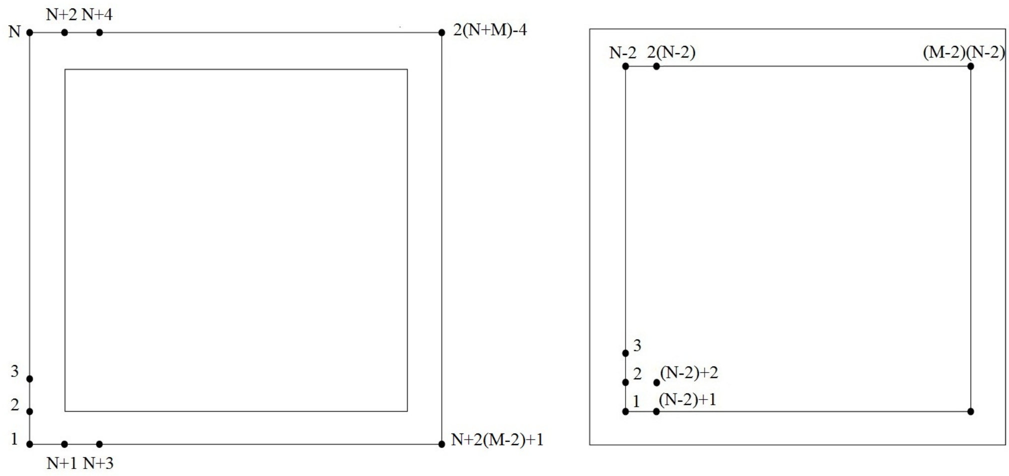

Figure A.1 The geometry of mash plate

$$\begin{bmatrix} B^k \\ D^k \end{bmatrix} \left\{ \vec{X} \right\} = \Omega^2 \left[\bar{I} \right] \left\{ \vec{X} \right\} \tag{A1}$$

The vector $\left\{ \vec{X} \right\}$, appeared in Eq. (A1), denotes the translational and rotational displacements of an imaging coordinate frame attached to the grid points. It is composed of the vectors d_B and d_D as equcetion.

The matrix $\left[\bar{I} \right]$ is a quasi-identity matrix equal to $\begin{bmatrix} 0 & 0 \\ 0 & I \end{bmatrix}$ appeared in Eq. (A1).

B^k and D^k in the equation represent the weighting coefficients of the components of $\left\{ \vec{X} \right\}$ in the k^{th} boundary condition and in the k^{th} domain equation respectively ,for constructing according to differential quadrature technique.

The equation (A1) might be rewritten as equation (A2).

$$\begin{bmatrix} \text{BB} & \text{BD} \\ \text{DB} & \text{DD} \end{bmatrix} \left\{ \begin{array}{c} d_B \\ d_D \end{array} \right\} = \Omega^2 \left[\bar{I} \right] \left\{ \begin{array}{c} d_B \\ d_D \end{array} \right\} \tag{A2}$$

In Eq. (A2) BD, DB are created due to the fact that the domain and boundary equations are coupled with each other.

These matrices BB and DD come into existence after assembling of the difference equations of the domain and boundary of the plate. The grid points of the domain and the boundary have been illustrated in Figure A.1.

$$d_B = \begin{bmatrix} X_1^B & \ldots & X_{2(N+M)-4}^B \end{bmatrix}^{\mathrm{T}} \tag{A3}$$

$$d_D = \begin{bmatrix} X_1^D & \ldots & X_{(N-2)(M-2)}^D \end{bmatrix}^{\mathrm{T}} \tag{A4}$$

$$X_i^B \text{ and } X_i^D \equiv \begin{bmatrix} \Theta_{x_i} & \Theta_{y_i} & W_i \end{bmatrix}^{\mathrm{T}} \tag{A5}$$

$$\left\{ \vec{X} \right\} = \begin{bmatrix} d_B & d_D \end{bmatrix}^{\mathrm{T}} = \begin{bmatrix} X_1^B & \ldots & X_{2(N+M)-4}^B \,|\, X_1^D & \ldots & X_{(N-2)(M-2)}^D \end{bmatrix}^{\mathrm{T}} \tag{A6}$$